Vol. 17: 19–31, 2001 | CLIMATE RESEARCH Clim Res | Published July 4

Pasture responses to elevated temperature and doubled CO_2 concentration: assessing the spatial pattern across an alpine landscape

M. Riedo[1,*], D. Gyalistras[2], J. Fuhrer[1,]**

[1]Swiss Federal Research Station for Agroecology and Agriculture (FAL), Liebefeld, 3003 Bern, Switzerland
[2]Institute of Geography, University of Bern, 3012 Bern, Switzerland

ABSTRACT: Climatic change and increasing atmospheric CO_2 concentration are expected to have significant effects on grassland ecosystems, but the magnitude of the responses may vary strongly across complex landscapes. A combination of the mechanistic pasture simulation model PaSim, statistical interpolation of climate parameters, and stochastic weather generation was used to examine the range and spatial distribution of the long-term responses of grazed grassland ecosystems to step changes in temperature and CO_2 across the 250 km^2 alpine Davos/Dischma region in Switzerland. 750 sites were considered, covering an altitude range from 1500 to 2700 m above sea level. PaSim was driven with site-specific hourly weather data, georeferenced input data for topography, and soil and vegetation characteristics. A seasonally uniform temperature increase by 2°C raised the mean evapotranspiration (*ET*) from about 200 to 300 mm yr^{-1}, and net primary production (*NPP*) from about 0.2 to 0.3 kg C m^{-2} yr^{-1}. Doubling CO_2 to 700 ppm partially offset the increase in *ET*, but caused an additional increase in *NPP*. The effects of the different scenarios on the simulated mean labile soil organic carbon content (C_{fast}) were small, and on the order of +1 % due to increased temperature and +5 % due to increased CO_2. Largest absolute changes in *ET* were obtained for sites with ample precipitation, whereas relative changes correlated best with altitude. Largest absolute changes in *NPP* were obtained for the most productive lower sites, whereas at higher sites absolute changes became small, but relative changes were again largest. Most pronounced increases in C_{fast} of around 10 % (equivalent to about 0.3 kg C m^{-2}) resulted from the combined temperature and CO_2 increase and occurred mainly at the higher elevation sites. For all parameters examined the variability of absolute system responses across sites was generally larger than the magnitude of the mean changes resulting from any scenario. Statistical analysis of the relationship between a small set of site-specific input parameters and model outputs revealed that the most important factors determining absolute system responses under all scenarios were altitude and aspect for *ET*, temperature for *NPP*, and soil texture (i.e. clay fraction) for C_{fast}. Absolute and relative changes due to the assumed changes in CO_2 and/or temperature depended less clearly on these factors, in particular for C_{fast}. These results show that the interaction of the effects of elevated CO_2 and increased temperature with local site conditions causes a spatially inhomogeneous distribution of grassland responses in a topographically complex landscape, but that absolute system responses for a given temperature and CO_2 regime can be explained with very high accuracy by a small number of environmental variables.

KEY WORDS: Alpine grassland · Climate change · Elevated CO_2 · Environmental modeling · Evapotranspiration · Net primary productivity · Soil carbon

1. INTRODUCTION

Grasslands cover a large fraction of the landscape in the European Alps. They vary in vegetation character-

*Present address: Centre for Ecology and Hydrology (CEH) Edinburgh, Bush Estate, Penicuik, Midlothian EH26 0QB, United Kingdom
**Corresponding author. E-mail: juerg.fuhrer@iul.admin.ch

istics and productivity according to soil, topography, climate, and management. Future climate warming with associated changes in precipitation, as projected for the Alpine region under increasing concentrations of greenhouse gases (Gyalistras et al. 1998, Gyalistras 2000) may effectively alter the conditions for grasslands, but the pattern of change across complex landscapes may be patchy. Differential effects along sharp gradients in climate and altitude may lead to a changed spatial distribution of productivity, which could be of socio-economic importance (Behringer et al. 2000).

Climate change (CC), in combination with increased atmospheric CO_2, may directly or indirectly affect grassland productivity (Riedo et al. 1999, Nösberger et al. 2000), and these effects are related to changes in the system carbon (C) and nitrogen (N) dynamics (Coughenour & Chen 1997). A change in C dynamics is important because grassland soils are important C sinks (see IPCC 2000). CC may cause a net loss of soil C, as opposed to an increase in C sequestration due to the direct effect of elevated CO_2 (Hunt et al. 1991, Ojima et al. 1993, Parton et al. 1994). At present, the outcome of the interaction between these factors is uncertain. Based on historical data, Tian et al. (1999) using the Terrestrial Ecosystem Model (TEM) showed that during 1900–1994 the effects of climate variability and CO_2 on soil C in the conterminous USA were not additive. Riedo et al. (2000) concluded that in response to CC and elevated CO_2 grassland soil C may either be increased or decreased depending on location and management. A better understanding of the response of soil C to altered environmental conditions could help to develop management strategies for the protection of soil C stocks (IPCC 2000).

Effects of CC and elevated CO_2 on grasslands have been analyzed with biophysical models at various spatial scales. At the global scale, a stimulation of net primary productivity (*NPP*) under moist temperate conditions was found to be the result of the stimulating effect of increased temperature on soil N availability (e.g. Mellilo et al. 1993). However, studies at the global scale offer little information about possible effects at smaller scales which are of interest to decision makers and practitioners. In addition, it is unclear how global models are capable of reproducing even the real mean response of grasslands in a topographically complex situation. The effects of CC and elevated CO_2 on grasslands is influenced by local site conditions (Riedo et al. 1999). Variations in site factors, such as soil type, aspect, or altitude could thus cause important spatial heterogeneity in grassland responses to CC and elevated CO_2 across a landscape. An increase in seasonal evapotranspiration (*ET*) combined with increased productivity has been identified for sites without soil moisture limitation; in contrast, drier and warmer sites have experienced an increase in water use, leading to soil water limitations and declining productivity (Riedo et al. 1999). According to Rounsevell et al. (1996) and Riedo et al. (2000) grassland on good quality land at higher altitudes may benefit relatively more than grasslands at lower sites or sites on less favourable land.

Increasingly, ecosystem models are spatially explicit, relying on spatially distributed and georeferenced data as model inputs; thus they can be used to assess the spatial patterns in ecosystem responses (Burke et al. 1990). The approach depends on the availability of data derived from geographical information systems (GIS) data layers, which have varying degrees of uncertainty associated with them. Thus, the most important inputs for which the highest precision is needed must be identified. Using different data sets for temperature, precipitation, solar radiation, and soil texture, Pan et al. (1996) found that with respect to *NPP* estimates the impact of uncertainty associated with soil texture data is most important and that the uncertainty is more important at the smaller compared to the larger scales. Alternatively, the importance of different inputs could be assessed by analyzing their statistical relationships with process-model outputs using data for a large number of sites.

In the present study, we used the well-tested, mechanistic Pasture Simulation Model (PaSim) (Riedo et al. 1998, 2000) in combination with the stochastic weather generator WeathGen (Gyalistras et al. 1997, Gyalistras & Fischlin 1999) to investigate the factors controlling pasture responses to CC and elevated CO_2 across a representative case study region in the Swiss Alps. In a 2-step procedure, the aim was (1) to quantify the spatial variability of *NPP*, *ET* and labile soil C stocks under the assumption of a step change in CO_2 ($2 \times CO_2$) and temperature, singly and in combination, and (2) to identify the relative importance of a small set of local site factors in determining the magnitude of the respective response by a statistical analysis of PaSim outputs.

2. MATERIAL AND METHODS

2.1. Study area. The chosen area of Davos with the Dischma valley is located at 46.8° N, 9.8° W in the eastern part of the Swiss Alps (Fig. 1) at the border between the more humid northern Alps and the drier central Alps. The surface of the selected area is roughly 250 km^2. The altitude across the area extends from 1500 m at the bottom of the main valley to 3200 m above sea level (asl). The main soil types are brown soil, brown podzols, and podzols. Grasslands suitable for agricultural production cover 41% of the area (Wildi & Ewald 1986).

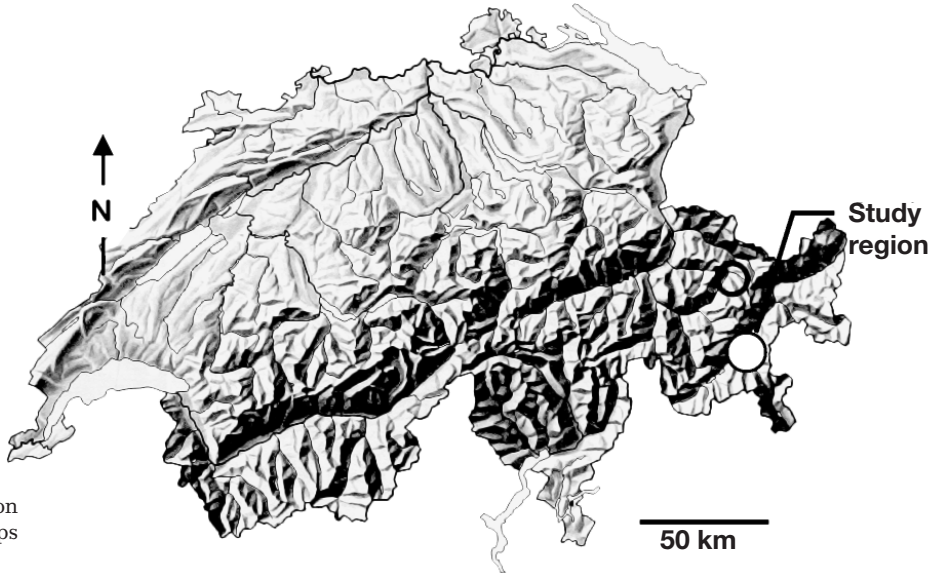

Fig. 1. Location of case study region Davos/Dischma in the Swiss Alps

2.2. Data. Data from 3 sources were used: (1) A 50 m × 50 m GIS database with a digital terrain model and information on land use and soil characteristics which was built in the framework of the UNESCO programme Man and Biosphere (MAB) (Wildi & Ewald 1986) was utilized. A subset of 750 sites was extracted to obtain a grid with a resolution of 200 m. Sites with one of the following vegetation types were identified: productive meadows, subalpine unimproved meadows, subalpine pastures, and alpine meadows on acid soils. Statistical characteristics of the selected subset are given in Table 1. (2) Hourly and daily weather records from the meteorological station Davos and daily data from 10 stations in the surroundings of the study region were provided by the Swiss Meteorological Institute (Bantle 1989, 1993) and for the site Stillberg in the Dischma valley by the Swiss Federal Institute for Forest, Snow and Landscape Research (Schönenberger & Frei 1988). (3) Standard parameter settings of the ecosystem model (Riedo et al. 1998, 2000).

2.3. Simulation tools. ***2.3.1. Ecosystem model:*** PaSim version 2.5 (Riedo et al. 2000) was used. The model is driven by hourly data for temperature (T_a), precipitation (P), global radiation ($I_{ATM,tot}$), vapour pressure (vp) and wind speed (u). PaSim 2.5 was adapted to use *Slope* (radian) and *Aspect* (radian) as site-specific input parameters. In the microclimate submodel, the canopy radiation profile was calculated for parallel layers, and the energy balances for canopy and soil were calculated for energy fluxes perpendicular to the soil surface. $I_{ATM,tot}$ (W m^{-2}) is given per unit area of the virtual horizontal layer and is the sum of the direct solar radiation, $I_{ATM,direct}$ (W m^{-2}), and the diffuse radiation, $I_{ATM,diffuse}$ (W m^{-2}). The direct solar radiation perpendicular to the soil surface, $I_{ATM,direct,slope}$ (W m^{-2}), is given by

$$I_{ATM,direct,slope} = I_{ATM,direct}\cos(\theta)/\cos(Zenith) \quad (1)$$

where *Zenith* (radian) is the zenith angle of the sun and θ (radian) is the angle between the sun and the normal to the soil surface, which depends on *Slope*, *Aspect* and the zenith and azimuth angles of the sun. The diffuse radiation perpendicular to the soil surface, $I_{ATM,diffuse,slope}$ (W m^{-2}), is calculated as

$$I_{ATM,diffuse,slope} = I_{ATM,diffuse}(\cos[Slope/2])^2 \quad (2)$$

In the soil physics submodel, the soil temperature (T_{soil}) profile was calculated for layers parallel to the soil surface.

Table 1. Statistical description of the 750 selected sites in the Davos/Dischа region. masl: meters above sea level

Statistics	Slope (degrees)	sin(aspect)	cos(aspect)	Altitude (masl)	Rooting depth[a]	Soil texture[a]	Annual mean temperature (°C)	Annual precipitation (mm)
Minimum	0.7	−1.0	−1.0	1530	0	0	−1.7	964
5% percentile	4.4	−0.990	−0.990	1575	0	0	−1.5	983
Mean	20.5	0.134	−0.147	2155	1.61	0.868	0.4	1144
95% percentile	37.0	0.995	0.914	2520	3	3	3.3	1246
Maximum	48.4	1.0	1.0	2690	3	3	3.6	1258

[a]The GIS database considers 4 levels of rooting depth (see Table 2) and 4 indices for soil texture (see Table 4)

2.3.2. Stochastic weather generation and climate interpolation: Site-specific hourly weather inputs were generated according to the method of Gyalistras & Fischlin (1999). The method was implemented with the aid of the stochastic weather generator WeathGen (version 2.6.1) (Gyalistras et al. 1997) and the ClimShell software (version 1.6a) (Gyalistras & Fischlin 1995, Fischlin & Gyalistras 1997).

WeathGen generates for each day the necessary hourly inputs $\boldsymbol{H}_{(s,y,m,d,h)}$ (where s, y, m, d and h denote a given site, year, month, day and hour, respectively) based on a parameter vector $\boldsymbol{\kappa}_{(s,m)}$ and a daily input vector $\boldsymbol{D}_{(s,y,m,d)}$. The latter is given by the following 11 weather statistics: (1) daily total P, (2) daily mean $I_{\mathrm{ATM,tot}}$, and (3–11) daily mean, minimum and maximum T_a, vp, and u. $\boldsymbol{D}_{(s,y,m,d)}$ is in turn generated for each month based on a parameter vector $\boldsymbol{\lambda}_{(s,m)}$ and a monthly input vector $\boldsymbol{M}_{(s,y,m)}$. This vector consists of the following 22 monthly weather statistics: (1) the probability of a wet day, π, (2) the monthly total P, and (3–22) the monthly means and within-month standard deviations of daily mean $I_{\mathrm{ATM,tot}}$ and of daily mean, minimum and maximum T_a, vp, and u.

Both transitions, from monthly to daily and from daily to hourly weather, are based upon first-order Markov chain-exponential models to simulate P and first-order auto-regressive models to simulate all other variables conditional on P. Parameter vectors $\boldsymbol{\kappa}_{(s,m)}$ and $\boldsymbol{\lambda}_{(s,m)}$ contain the site- and month-specific stochastic process parameters, which are a series of parameters that are used to empirically predict some of the process parameters from the respective inputs (for instance, the daily transition probabilities between wet and dry days for a given month are determined based on that particular month's wet-day probability π). To ensure consistency among temporal aggregation levels, WeathGen repeatedly simulates daily (or hourly) weather sequences until the statistics of a simulated sequence for a given month (day) are sufficiently close to the respective monthly (daily) inputs. Finally, an accepted weather sequence is adjusted such that its statistics exactly reproduces the respective inputs. The use of monthly data with WeathGen has been shown to enable an accurate estimate of annually averaged PaSim outputs (Gyalistras et al. 1997).

The monthly inputs $M_{i(s,y,m)}$ (i = 1 … 22) were interpolated at each site according to

$$M_{i(s,y,m)} = m_{i(s,m)} + \Delta m_{i(\mathrm{Davos},y,m)}$$

where $m_{i(s,m)}$ denotes the interpolated long-term mean of variable M_i at site s and for month m, the subscript Davos refers to the corresponding meteorological station, and $\Delta m_{i(\mathrm{Davos},m,y)}$ is $M_{i(\mathrm{Davos},y,m)} - m_{i(\mathrm{Davos},m)}$. Note that according to this procedure all interpolated time series have the same variability as the measurements in Davos, i.e., we did not consider any possible site or altitudinal dependencies of the higher-order moments of the M_i.

To estimate a given $m_{i(s,m)}$, a linear regression was first applied to predict this value from elevation and then the result was adjusted based upon an inverse distance-weighted (IDW) interpolation of elevation-detrended values (i.e., of the regression residuals) from surrounding stations (Gyalistras & Fischlin 1999). Regression parameters were estimated using data from all stations within a search radius R around the target site. For monthly P sums, for which a dense network of climate stations was available, R was 5 km; for all other monthly inputs R was 10 km. The same R was used for IDW, and the weight of an individual station was given as (1/distance).

The parameter vectors $\boldsymbol{\kappa}_{(s,m)}$ and $\boldsymbol{\lambda}_{(s,m)}$ are very large (several hundreds of values per month, Gyalistras et al. 1997) and therefore no interpolation was applied. Instead we used at all sites the parameter values from Davos.

2.4. Parameter values. ***2.4.1. Topographic and climatic parameters:*** *Altitude* (m), *Slope* (radian), and *Aspect* (radian) for each site were extracted from the GIS database. All parameters of the weather generator were estimated from hourly data for Davos for the period 1981–1985. The 22 monthly weather inputs were derived from daily data for 1971–1994. Further details on data preparation have been given elsewhere (Gyalistras et al. 1997). Interpolation of all $m_{i(s,m)}$ was performed for the 1931–1980 baseline, with the exception of the expected values related to u. Due to lack of data, the latter were determined for the baseline 1971–1990.

Long-term measurements that covered the baselines were available at several stations only for monthly mean T_a and monthly total P. For all other variables long-term data were available only at Davos. Therefore, where possible, prior to interpolation station records were extended to cover the entire baseline period. This was accomplished with the aid of the ClimShell software as follows: First we searched, separately for each climate station, month, and variable M_i, the long-term climate station for which the correlation between the 2 M_i time series from the 2 stations was maximized. Only station pairs with at least 15 yr (monthly total P) or 5 yr (all other variables) of common data were considered. Then the record at the target station was extended based on a linear regression from the long-term station found.

This procedure resulted into a varying station network, depending on the variables considered: For interpolation of the m_i related to vp, only data from 2 stations were available (Davos and Weissfluhjoch). For all other variables we used in all cases 1 further station

(Stillberg); for monthly mean T_a and monthly total P, in addition to Stillberg, 2 and 13, respectively, further stations in the vicinity of the Dischma valley were used.

2.4.2. Ecosystem model input parameters: Hourly weather data were generated as described above. Most of the other PaSim input parameters could be derived from the GIS database, or were estimated from other sources, as described below. For the remaining input parameters, standard settings obtained from other Swiss grassland sites were used (Riedo et al. 1998).

Grazing by lactating cows was used as the only management option. The stocking density of lactating cows was varied each day in such a way that the leaf area index of the sward remained near the value of 2 m^2 m^{-2} during the growing season. Animal live weight was assumed to be 600 kg, and the potential intake rate was set to 14 kg dry weight $ind.^{-1}$ d^{-1}.

The number and depth of the soil layers and the depth of the groundwater level were derived from the GIS database with 4 levels of the rooting depth and 4 levels of soil wetness. The number and depth of soil layers were determined from rooting depth according to Table 2, but in cases where one of the levels of soil wetness was available, the number of soil layers was reduced so that the deepest soil layer was above the groundwater level, as derived from soil wetness according to Peyer & Frei (1992) (Table 3). The depth of the soil boundary layer was set to the groundwater level if soil wetness was available (Table 3). If not, it was assumed that there was no groundwater level, and the depth of the soil boundary layer was determined from rooting depth (Table 2). Soil texture, i.e., the fractions of sand, silt, and clay, was derived from the 4 levels given in the GIS database (AG Boden 1994) (Table 4). The calculation of the remaining input parameters is described in Appendix 1.

2.4.3. Ecosystem model initial values: The initial condition for root dry matter was calculated as a function of the actual forage yield and the vegetation unit, as derived from the GIS database. The following yield to root dry matter ratios were assumed: 1 to 2 for productive sites and 1 to 4 for unimproved sites (von Wyl 1987).

Table 2. Relationship between soil layers considered in the PaSim simulations and rooting depth levels in the GIS database

Level	Rooting depth (m)	Soil layers (m) 1	2	3	4	5	6	Boundary
0	>0.50	0.02	0.05	0.1	0.2	0.4	0.7	0.75
1	0.3–0.5	0.02	0.05	0.1	0.2	0.4		0.45
2	0.1–0.3	0.02	0.05	0.1	0.2			0.45
3	<0.1	0.02	0.05	0.1				0.45

Table 3. Relationship of the number of soil layers and groundwater level considered in the PaSim simulations with the soil wetness factor in the GIS database

Soil wetness	Number of soil layers	Groundwater level (m)
Slightly wet	≤6	0.75
Wet	≤5	0.45
Very wet	≤4	0.25
Swamp	≤3	0.15

Table 4. Relationship between sand/silt/clay fractions considered in the PaSim simulations for the soil texture index in the GIS database and soil type according to AG Boden (1994)

Soil texture index	Sand (%)	Silt (%)	Clay (%)	Soil type
0	90	5	5	Sand (Ss)
1	63	25	12	Loamy sand (Sl3, Sl4)
2	49	30	21	Sandy loam (Ls3, Ls4)
3	20	40	40	Clay loam (Lt3)

For the simulation with present-day climate and CO_2 the initial conditions for C and N in different soil organic pools for site 1 were set to the equilibrium values calculated for Davos (Riedo et al. 2000). For site n, values obtained for site $n-1$ after 48 yr of simulation were used. With changed climatic and/or CO_2 conditions, initial conditions for C and N were set to values obtained at the end of the respective 48 yr reference simulation at the same site. For the remaining initial conditions, standard values were used (Riedo et al. 1998).

2.5. Simulation experiments. Four simulations were carried out: (1) Current: reference run using present-day (1931–1980) climate and 350 ppm CO_2; (2) $2 \times CO_2$: present-day climate and 700 ppm CO_2; (3) ΔT: increase in T_a by 2°C and 350 ppm CO_2; (4) $2 \times CO_2 + \Delta T$: increase in T_a by 2°C with 700 ppm CO_2.

PaSim was driven by 48 yr of hourly weather data obtained as follows: (1) WeathGen was used to simulate 24 yr of site-specific hourly data. (2) The data were recycled to obtain a 48 yr record. (3) For ΔT and $2 \times CO_2 + \Delta T$, WeathGen inputs were adjusted by adding 2°C to the monthly input time series for daily mean, minimum, and maximum T_a, while the diurnal course and within-month or year-to-year variability of T_a were left unchanged. All other monthly input variables and climate parameters were used as described above (Section 2.3).

The following model outputs were considered: *NPP* (kg C m^{-2} yr^{-1}), *ET* (mm yr^{-1}), and the total of the soil organic C (SOC) in the system which is in the labile and not in the passive pool, C_{fast} (kg C m^{-2}). Values for *NPP* and *ET* represent the yearly cumulative flux, and for C_{fast} the C content at the end of a year.

2.6. Statistical analysis. The relationships between model outputs and selected site factors were investigated by multivariate regression analysis. The averages of the model outputs from the last 24 yr of the 48 yr simulations were considered. We used the absolute ($\Delta Y = Y_{new} - Y_{ref}$, where Y = *NPP*, *ET* or C_{fast}) and relative [$\Delta Y\% = 100\ (Y_{new} - Y_{ref})/Y_{ref}$] differences between results from reference runs (Y_{ref}) and runs under changed conditions (Y_{new}). Because *ET*% and *NPP*% were strongly positively skewed, they were used after log-transformation. Eight site-specific parameters X_i (i = 1 … 8) were used to describe environmental conditions: slope, sine and cosine of aspect, altitude, rooting depth, texture, annual P sum, and annual mean T_a. Values of X_i were standardized to zero mean and unit variance such that they entered the subsequent analysis with equal weights. Finally, for each Y or ΔY% we determined optimal multivariate linear regression models to predict this variable from a subset of X_i. Due to the standardization of X_i, the coefficient b_i in a given regression equation Y or $\Delta Y\% = a + b_i X_i$ represents the system response per unit standard deviation change in a given X_i.

The optimal regression model used a minimum number of predictors, but still maximized r^2; S-PLUS Software (Statistical Sciences 1995) was used with stepwise addition or removal of predictors. The former retained 3 to 8 (all) predictors, whereas the latter yielded more parsimonious models (2 to 6 predictors) with only small reductions in model performance (r^2 smaller by typically less than 1%). We report only results obtained with stepwise addition.

3. RESULTS

3.1. Variability in grassland responses

The range and the frequency distribution of *ET*, *NPP* and C_{fast} across the 750 selected grassland sites were similar under current and changed climatic and/or CO_2 conditions, as shown by the box plots (Fig. 2a). Compared to the reference simulation, areal mean *ET* was slightly lower with $2 \times CO_2$, and higher for *NPP* and C_{fast}. The increment in T_a by 2°C caused an increase in *ET* from about 200 to 300 mm yr^{-1}, and *NPP* was stimulated from about 0.2 to 0.3 kg C m^{-2} yr^{-1}. $2 \times CO_2$ partially offset the increase in *ET* induced by ΔT, but this scenario caused an additional increase in *NPP*. The effect of the different scenarios on C_{fast} was relatively small. For *NPP*, *ET* and C_{fast} the variability was generally larger than the magnitude of the mean changes resulting from any scenario. The largest relative changes were found for *NPP* in response to the combination of $2 \times CO_2$ and ΔT, and for *ET* in response to ΔT. Much smaller relative changes were found for C_{fast}; with $2 \times CO_2$ C_{fast} increased for the majority of sites by <10%, whereas ΔT had small and variable effects on C_{fast}. In response to $2 \times CO_2 + \Delta T$, mean C_{fast} increased by about 5%.

3.2. Distribution of grassland responses

To obtain a visual picture of the spatial distribution of the grassland responses to the combined $2 \times CO_2 + \Delta T$ scenario, the absolute and relative changes obtained

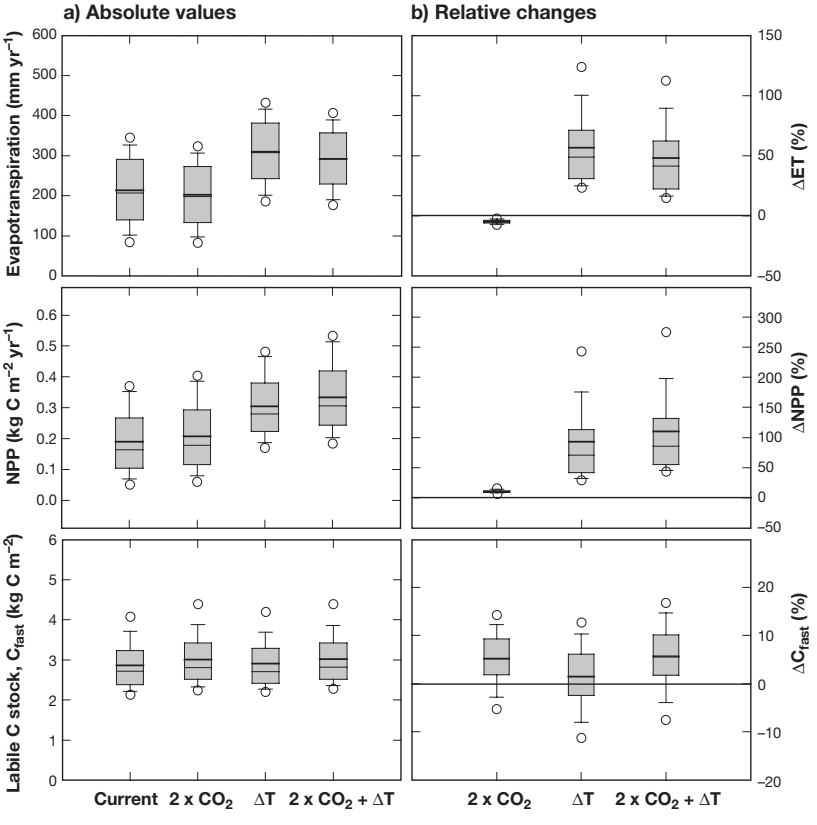

Fig. 2. Variability in the (a) absolute and (b) relative responses of *ET*, *NPP* and C_{fast} to doubled CO_2 ($2 \times CO_2$), increased temperature (ΔT) and a combination ($2 \times CO_2 + \Delta T$). The box plots show the mean and median with 10th, 25th, 75th and 90th percentiles as vertical boxes with error bars. Circles: total range

for each selected site were plotted in combination with a 3-D presentation of the topography. The spatial pattern of the *NPP* response showed that the relative change increased with altitude, i.e., largest relative *NPP* stimulation of >100% was obtained for the high-altitude, low-productivity meadows (Fig. 3a). In contrast, largest changes in absolute terms were obtained for the most productive sites located at the bottom of the valley with increases >0.15 kg C m^{-2} yr^{-1} (Fig. 3b). A similar spatial visualization was carried out for C_{fast}. The plot for relative changes in C_{fast} shows less of a consistent trend with altitude, as compared to *NPP* (Fig. 4a), and the distribution of absolute changes indicates only a weak relationship between the relative changes in C_{fast} and *NPP* (Fig. 4b). Unlike in the case of *NPP*, for which similar changes were obtained for both aspects, a clear difference between the changes in C_{fast} on the 2 mountain ridges (Jakobshorn vs Schwarzhorn) appeared in the plot, indicating the influence of factors other than altitude on the response of C_{fast}.

3.3. Regression analysis

Regression analysis with stepwise addition of predictors revealed the most important factors determining the

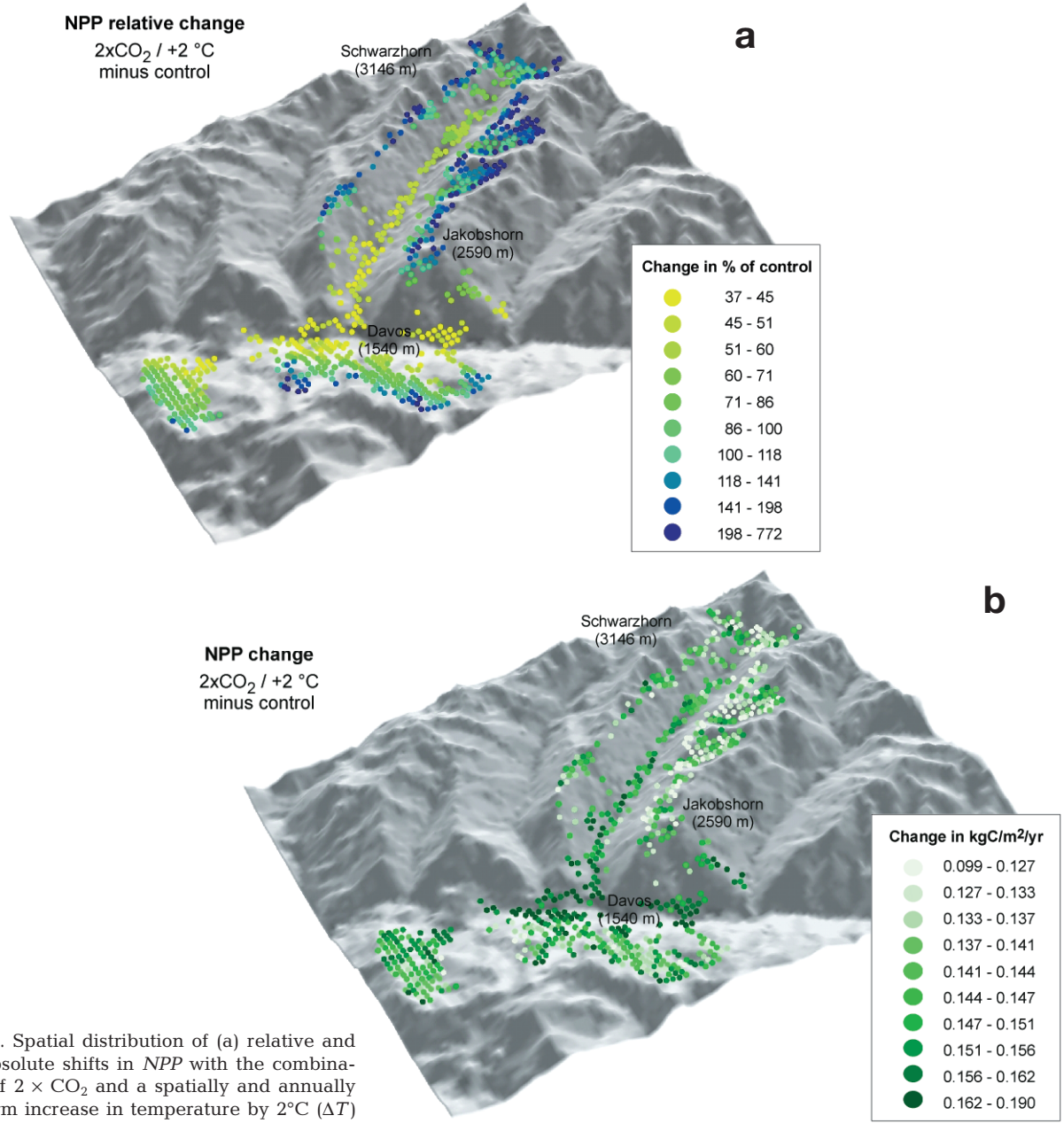

Fig. 3. Spatial distribution of (a) relative and (b) absolute shifts in *NPP* with the combination of 2 × CO_2 and a spatially and annually uniform increase in temperature by 2°C (ΔT)

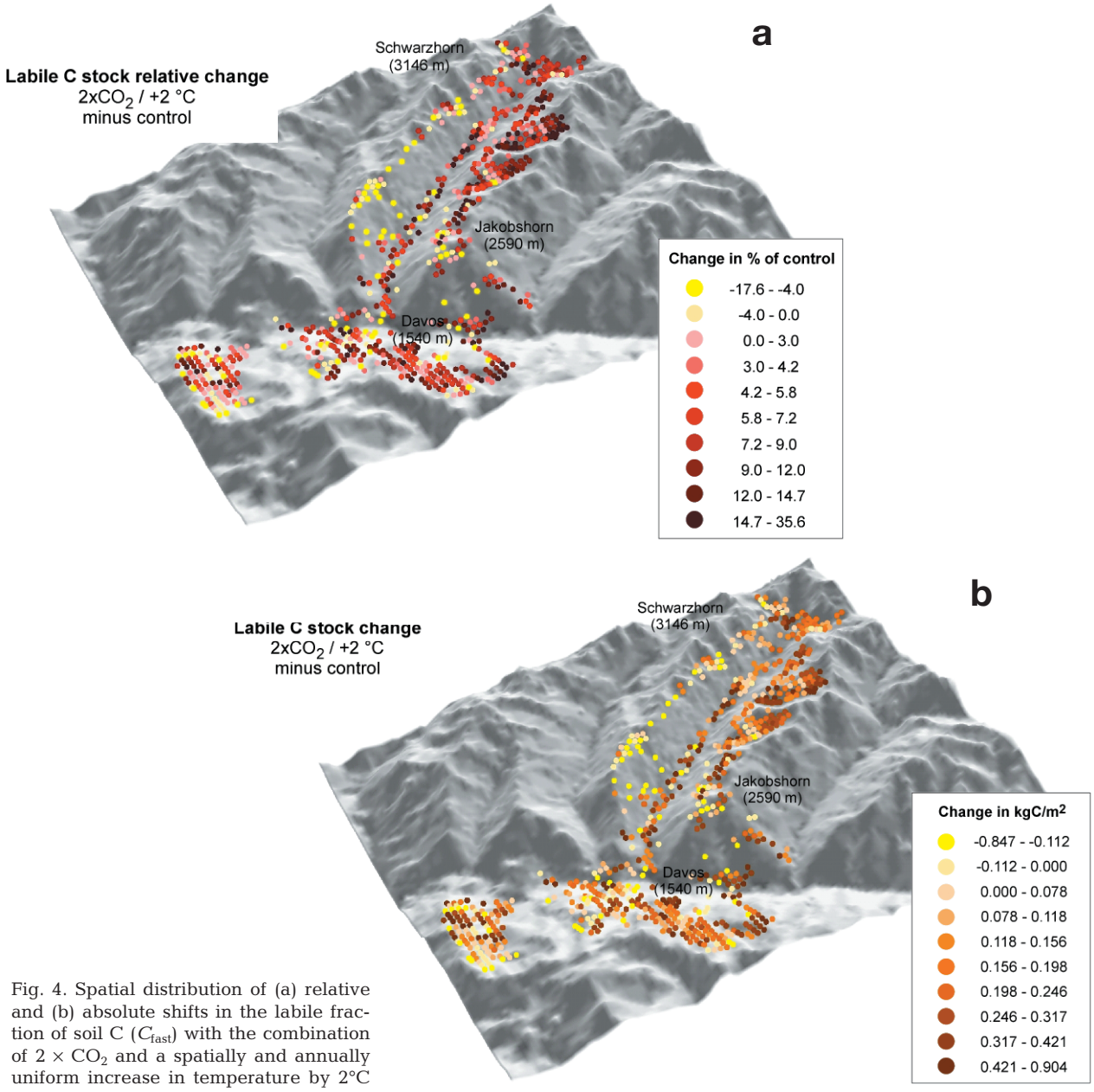

Fig. 4. Spatial distribution of (a) relative and (b) absolute shifts in the labile fraction of soil C (C_{fast}) with the combination of 2 × CO_2 and a spatially and annually uniform increase in temperature by 2°C

spatial variability of absolute system responses. The most important factors are identified by the largest change per unit standard deviation. These were *Altitude* for *ET*, T_a for *NPP*, and *soil texture* for C_{fast} (Fig. 5a). The relationship of *ET* with *Altitude* was negative, while soil texture and T_a were positively related to C_{fast} and *NPP*, respectively. Higher values for soil texture represent soils with increasing clay and silt fractions, and a decreasing sand fraction. Relative changes in the response to 2 × CO_2 or ΔT were generally less well explained by linear models (Fig. 5b). The relative change in *ET* was positively influenced by *Altitude*, and the change in *NPP* negatively by T_a. C_{fast} was positively related to both altitude and T_a, and to a lesser extent to soil texture.

4. DISCUSSION

The interaction between the effects of 2 × CO_2 and/or increased T_a (ΔT) with local site conditions causes a spatially inhomogeneous distribution of the grassland responses across this alpine landscape. This is plausible, since it is well known that elevated CO_2 effects on plants are influenced by water and nutrient availability and that relative responses tend to be larger under conditions of limited resources (see Idso & Idso 1994). In agreement, the largest absolute changes in *NPP* were obtained for the most productive sites (Fig. 3), whereas at higher sites, i.e., near the limit for grassland production, absolute changes become small, but rela-

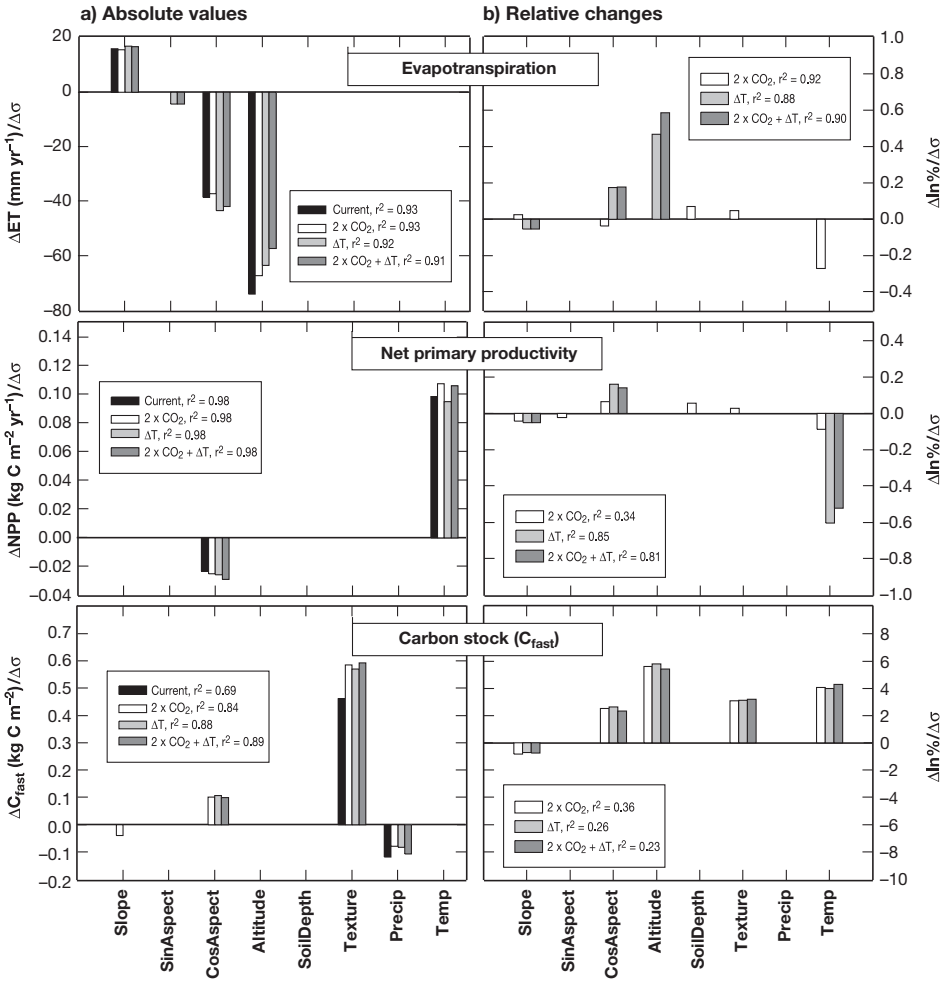

Fig. 5. Response of *ET*, *NPP* and C_{fast} per standard deviation change in the respective environmental factor for (a) absolute and (b) relative values. The magnitude of the bar is an indication of the importance of the respective input

tive changes are largest. This general trend confirms results obtained for upland and lowland sites in Britain (Thornley & Cannell 1997). The vertical differentiation in absolute productivity changes could have practical implications. For instance, the area under production could be reduced to the most productive areas, while marginal grassland sites would be abandoned in the absence of economic incentives (Behringer et al. 2000). But, even at similar altitudes, sites-specific responses may differ because of differences in nutrient availability, soil characteristics, or microclimatic differences.

The range of simulated *ET* under current conditions agrees well with measured data from alpine sites (Rosset et al. 1997), and the stimulation of *ET* with $2 \times CO_2$ and ΔT agrees with results from previous simulations for wet sites (Riedo et al. 1997). These results confirm that under the conditions prevailing in the alpine region a reduction in leaf transpiration with $2 \times CO_2$ is more than compensated for by the stimulation by higher T_a (Riedo et al. 2000). The variability in the response of *ET* to $2 \times CO_2 + \Delta T$ was mainly determined by *Altitude* (Fig. 5). With decreasing T_a, corresponding to increasing altitude, the modelled CO_2 responsiveness of photosynthesis declines, while the plants' sensitivity to temperature increases (Riedo et al. 1999). Hence, at higher altitudes effects of changed T_a, as the most important factor influencing *NPP* (Fig. 5), dominate over the $2 \times CO_2$ effect on plant growth. The increase in growth, combined with stimulated *ET*, could lead to higher system water use, and, consequently, to reduced soil moisture. This negative feedback was demonstrated by Rounsvell et al. (1996) for upland areas in the UK. However, our simulations show that in the selected alpine region soil water availability is not becoming a limiting factor with an increase in T_a by 2°C combined with increased *ET*. With an annual *P* of 960 to 1260 mm (Table 1) and values of about 700 mm for the growing season (Rosset et al. 1997), the calculated *ET* of <400 mm remains below *P* even under the warmer conditions, and when taking into account a surface runoff of 3 to 5% of *P* (Prasuhn & Braun 1994). Clearly, the situation could change if a CC scenario with significantly reduced *P* were to be applied. Current scenarios for the Alps indicate spatially and seasonally complex patterns of changes in *P* in response to global warming (Gyalistras et al. 1998,

Gyalistras 2000); thus this situation merits further consideration.

The accumulation of SOC reflects the net ecosystem production, i.e., the balance between ecosystem primary productivity and decomposition. Changes in SOC have attracted interest because of their importance as a major source of system stability, and because of the need to protect or even increase soil C pools to counteract the raise in atmospheric CO_2 (Batjes 1998, IPCC 2000). The increase in *NPP* by 0.1 kg C m^{-2} yr^{-1} on average with $2 \times CO_2 + \Delta T$ (Fig. 2a) could be associated with increased SOC content, provided that net below-ground productivity increases as well. As shown by Rastetter et al. (1997), accumulation of soil C on the time scale of centuries is determined by the increase in total ecosystem N. In managed grasslands, typically N is not limiting and thus the conditions are favourable for C sequestration under elevated CO_2 (Cannell & Thornley 1998). However, in our simulations, changes in the labile C pool (C_{fast}) were small compared to the changes in *NPP*. The results indicate that C_{fast} declines at some sites by up to 10% with ΔT, in agreement with results from other studies (Parton et al. 1994, Thornley & Cannell 1997). With an increase in T_a by 5°C, Coughenour & Chen (1997) found a decline in SOC by 20 to 30%. The sites exhibiting soil C losses under changed conditions tend to be located in the productive lower-altitude valleys. However, at other sites in the study region, absolute C_{fast} increases with $2 \times CO_2 + \Delta T$. These sites occur at the higher altitudes, where the relative T_a response of *NPP* is largest (Figs. 4 & 5). Hence, at these sites the higher C input to the soil via increased *NPP* overcompensates for the loss of soil C resulting from faster decomposition. This indicates that the outcome of the balance between C input and C loss depends on the working point with respect to T_a. However, the relative change in C_{fast} in response to climate warming and/or elevated CO_2 is not related to a single site factor (Fig. 5b). The results suggest that a specific response results from the interaction of soil texture, altitude and T_a, and thus it is difficult to predict with linear regression models. The interactive effects of the various factors on C_{fast} appear to differ between the 2 mountain ridges; this can be related to the difference in topography. Whereas the slope facing south-west is more plain, the slope facing south-east includes at least 2 smaller valleys formed by streams. Apparently, inside these valleys conditions are more favourable for *NPP* and C storage, with slightly higher temperatures and earlier disappearance of snow cover, as compared to the slope at the opposite side of the valley. According to the regional soil map, current soils in these small valleys contain higher amounts of humus and differ in texture (Wildi & Ewald 1986). The most important factor determining C_{fast} under all scenarios was soil texture, thus confirming the relationship obtained by Burke et al. (1990). C_{fast} is positively related to increasing clay plus silt contents of the soil. It is known from field measurements that SOC content tends to be higher when C mineralization rates are reduced, such as in soils with a high clay or clay plus silt content (Hassink 1994). Clay-rich soils often occur at sites with high *P* (Burke et al. 1989), which is not indicated by the regression analysis, whereas the direct influence of texture is very clear (Fig. 5). Overall, the simulations reveal that for the majority of sites, in particular for cooler sites with soils high in clay content, C_{fast} increases by up to 10% in response to climate warming and/or elevated CO_2, which is equivalent to approximately 0.3 kg C m^{-2}. This increase is in contrast to the small net C loss predicted for humid temperate grasslands worldwide (Parton et al. 1994), but in agreement with results from simulations for grazed pastures (Thornley & Cannell 1997).

Overall, it can be concluded that the distribution of temperate grassland responses in a topographically complex landscape is spatially inhomogeneous, but that absolute system responses can be explained with very high accuracy by a small number of environmental variables.

5. CONCLUDING REMARKS

The approach used here allows the variability in system responses across an entire alpine landscape to be quantified; it relies on a mechanistic ecosystem model in combination with georeferenced data as inputs. This automated method is highly data-demanding, but it allows the most important site factors determining ecosystem responses to be identified (Fig. 5). However, the results are influenced by uncertainties in the input data sets. The precision of several site-specific parameters (e.g. the soil type, rooting depth, bulk density, etc.) was limited, and several uncertainties were introduced due to the natural variability of climate and the spatial interpolation of climatic parameters, in particular for solar radiation and wind speed parameters, and due to the higher-order moments of weather variables needed for stochastic weather generation. Moreover, PaSim includes several critical assumptions, such as the dependence on altitude of plant growth which was fitted to field observations (Riedo et al. 2000). Finally, because of a response time of C_{fast} of about 34 yr for the site Davos (Riedo et al. 2000), the restriction of the simulation experiments to 48 yr caused an uncertainty of up to about 10% in the absolute results of C_{fast}.

Due to the large number of inputs, it is difficult to assess the representativeness of our results for other regions. However, within the range of validity of the ecosystem model, there are several reasons why the results

can be considered qualitatively robust and applicable also to other cool temperate regions: (1) PaSim is a general grassland model and has been shown to perform well under a range of conditions (Riedo et al. 1998); the soil biology submodel is based on the CENTURY model, which has also been tested under a wide range of conditions (Burke et al. 1989, Gilmanov et al. 1997). (2) In this study, sensitivities were tested at a large number of sites covering a wide range of working points. (3) The year-to-year variability of climate by performing at each site simulations for a large number of years was accounted for. (4) As shown elsewhere (Gyalistras et al. 1997), the annual response of the ecosystem model can be estimated with good accuracy from monthly weather data.

The results from the regression analysis of local process-model outputs and selected inputs could be used to establish efficient statistical models of grassland responses to environmental factors. These models could be applied over larger areas to explore the sensitivity of key ecosystem properties to a variety of CC scenarios. Generally there was a good fit of the simple regression models, and more sophisticated and robust statistical models could readily be constructed. For more practical applications, a robust, overall picture of likely changes as obtained in the present study would be sufficient (Behringer et al. 2000). However, any such modelling efforts should take into consideration that the statistical relationships between environmental factors and system outputs depend on the working point chosen for both CO_2 and climate. This suggests that purely empirical approaches to project grassland responses to CC and elevated CO_2 would be of limited applicability.

Appendix 1. Calculation of ecosystem model input parameters

Soil water content, $\theta_s(h)$ ($m^3\ m^{-3}$), and soil hydraulic conductivity, $k_s(h)$ ($m\ d^{-1}$), are given by

$$\theta_s(h) = \theta_{s,sat}(h)\left(\frac{\psi_e(h)}{\psi(h)}\right)^{1/b(h)} \quad (A1)$$

$$k_s(h) = k_{s,sat}(h)\left(\frac{\psi_e(h)}{\psi(h)}\right)^{2+3/b(h)} \quad (A2)$$

and thus depend on the soil physical parameters, $\theta_{s,sat}(h)$ ($m^3\ m^{-3}$), the saturated volumetric water content, $\Psi_e(h)$ (m), the air entry water potential, $b(h)$, an empirical parameter, and $k_{s,sat}(h)$ ($m\ d^{-1}$), the saturated soil hydraulic conductivity. $\Psi(h)$ in Eqs. (A1) & (A2) is the matrix potential related to $\theta_s(h)$. $\theta_{s,sat}(h)$ is given by the sum of the field capacity, $\theta_{s,fc}(h)$ ($m^3\ m^{-3}$) (soil water potential, $pF \geq 1.8$) and the air capacity, $\theta_{s,ac}(h)$ ($m^3\ m^{-3}$) ($pF < 1.8$). $\theta_{s,fc}(h)$ and $\theta_{s,ac}(h)$ were calculated from soil bulk density, soil organic matter (SOM) content, and texture (AG Boden 1994). Due to lack of data, it was assumed that SOM content was 10% at all sites and that soil bulk density was 0.8 g dry soil cm^{-3} (Peterer 1985). To calculate $\Psi_e(h)$, 2 pairs of corresponding values of θ_s and Ψ, i.e., $\theta_{s,fc}$ and Ψ_{fc} for field capacity, and $\theta_{s,pwp}$ and Ψ_{pwp} for permanent wilting point ($pF \geq 4.2$), were included in Eq. (A1), and the resulting equations were solved for b and then set equal to each other, resulting in an equation for Ψ_e:

$$\ln(\Psi_e) = \frac{\ln(\Psi_{pwp})\ln(\theta_{s,sat}/\theta_{s,fc}) + \ln(\Psi_{fc})\ln(\theta_{s,pwp}/\theta_{s,sat})}{\ln(\theta_{s,pwp}/\theta_{s,fc})} \quad (A3)$$

$\theta_{s,pwp}(h)$ was derived from AG Boden (1994). The parameter b was calculated from Eq. (A1), replacing the pair of corresponding values of θ_s and Ψ with $\theta_{s,pwp}$ and Ψ_{pwp}, and solving for b. Saturated soil hydraulic conductivity $k_{s,sat}(h)$ was calculated from soil bulk density and texture (AG Boden 1994). The same values for soil parameters were used for all soil layers. The temperature of the soil boundary layer, $T_{soil,b}$, is given by

$$T_{soil,b} = T_{soil,b,mean} + T_{soil,b,amp} \cdot \sin(t_{julian} 2\pi/365 - T_{soil,b,phase}) \quad (A4)$$

where $T_{soil,b,mean}$, $T_{soil,b,amp}$, and $T_{soil,b,phase}$ are site-specific input parameters.

Table A1. Rooting profile considered in PaSim simulations

Number of soil layers	Constraints	$f_{root,a}$	$f_{root,b}$
6	75% above 0.1 m, 100% above 0.7 m	13.9	0.139
5	60% above 0.05 m, 100% above 0.4 m	18.3	0.183
4	70% above 0.05 m, 100% above 0.2 m	23.9	0.237
3	75% above 0.05 m, 100% above 0.10 m	24.7	0.220

These were calculated as a function of the long-term monthly means of T_a. $T_{soil,b,mean}$ is given by

$$T_{soil,b,mean} = T_{a.mean} + 2.1 \quad (A5)$$

where $T_{a,mean}$ is the average of the long-term monthly means of T_a. $T_{soil,b,amp}$ is calculated as

$$T_{soil,b,amp} = T_{a,amp}\exp(-z_{sb}\cos[\text{slope}]/z_d) \quad (A6)$$

where $T_{a,amp}$ is half the difference between the minimum and maximum of the long-term monthly means of T_a. The parameter z_d was set to 2 m, and z_{sb} (m) is the depth of the soil boundary layer. $T_{soil,b,phase}$ in Eq. (A4) is given by

$$T_{soil,b,phase} = z_{sb}\cos[\text{slope}]/z_d + T_{a,phase} + 5 \cdot 2\pi/365 \quad (A7)$$

where

$$T_{a,phase} = 107 \cdot 2\pi/365 \quad (A8)$$

The values 2.1 in Eq. (A5), 5.0 in Eq. (A7), 107.0 in Eq. (A8), and the value for z_d were derived from measurements (Rosset et al. 1997). The depth of the main rooting zone of the soil was set to 0.1 m for all sites (Peterer 1985). The rooting profile was approximated by the function

$$f_{root}(x) = f_{root,a}e^{-f_{root,b}x} \quad (A9)$$

where x is the depth below the soil surface. The parameters $f_{root,a}$ and $f_{root,b}$ were fitted as a function of the number of soil layers with the constraints given in Table A1. The clover fraction of the swards was set to 15% for all sites.

Acknowledgements. This work was supported by the Swiss National Science Foundation in the framework of the Priority Program Environment (5001-44597). The work contributed to the CLEAR project and to the GCTE Core Research Programme (Focus 3), which is part of IGBP. We thank F. Kienast (WSL) for providing access to MAB Davos GIS database and J. Boehm (WSL) for the Stillberg data.

LITERATURE CITED

AG Boden (1994) Bodenkundliche Kartieranleitung, 4th edn. E Schweizerbart Publishing Company, Stuttgart

Bantle H (1989) Programmdokumentation Klima-Datenbank am RZ-ETH Zürich. SMA Tech Report, Schweizerische Meteorologische Anstalt, Zürich

Bantle H (1993) Benützeranleitung zur Datenbank EPAD. SMA Tech Report Schweizerische Meteorologische Anstalt, Zürich

Batjes NH (1998) Mitigation of atmospheric CO_2 concentrations by increased carbon sequestration in the soil. Biol Fertil Soils 27:230–235

Behringer J, Bürki R, Fuhrer J (2000) Participatory integrated assessment of adaptation to climate change in alpine tourism and mountain agriculture. Integ Assess 1:331–338

Burke IC, Yonker CM, Parton WJ, Cole CV, Flach CV, Schimel DS (1989) Texture, climate, and cultivation effects on soil organic matter content in U.S. grassland soils. Soil Sci Soc Am J 53:800–805

Burke IC, Schimel DS, Yonker CM, Parton WJ, Joyce LA, Lauenroth WK (1990) Regional modeling of grassland biogeochemistry using GIS. Landscape Ecol 4:45–54

Cannell MGR, Thornley JHM (1998) N-poor ecosystems may respond more to elevated [CO_2] than N-rich ones in the long term. A model analysis of grasslands. Global Change Biol 4:431–442

Coughenour MB, Chen DX (1997) Assessment of grassland ecosystem responses to atmospheric change using linked plant-soil process models. Ecol Appl 7:802–827

Fischlin A, Gyalistras D (1997) Assessing impacts of climatic change on forests in the Alps. Global Ecol Biogeogr Lett 6:19–37

Gilmanov TG, Parton WJ, Ojima DS (1997) Testing the 'CENTURY' ecosystem level model on data sets from eight grassland sites in the former USSR representing a wide climatic/soil gradient. Ecol Model 96:191–210

Gyalistras D (2000) Klimaszenarien für den Alpenraum und die Schweiz: Neuester Stand und Vergleich. In: Wanner H, Gyalistras D, Luterbacher J, Rickli R, Salvisberg E, Schmutz C (eds) Klimawandel im Schweizer Alpenraum. vdf Hochschulverlag, Zürich, p 197–235

Gyalistras D, Fischlin A (1995) Downscaling: applications to ecosystems modelling. In: Proceedings of the 6th International Meeting on Statistical Climatology, Galway, Ireland, 19–23 June 1995. University College, Galway, p 189–192

Gyalistras D, Fischlin A (1999) Towards a general method to construct regional climatic scenarios for model-based impacts assessments. Petermanns Geogr Mittlg 143:251–264

Gyalistras D, Fischlin A, Riedo M (1997) Herleitung stündlicher Wetterszenarien unter zukünftigen Klimabedingungen. In: Fuhrer J (ed) Klimaänderung und Grünland. vdf Hochschulverlag, Zürich, p 207–276

Gyalistras D, Schär C, Davis HC, Wanner H (1998) Future Alpine climate. In: Debon P, Dahinden U, Davis H, Imboden DM, Jaeger CC (eds) Views from the Alps. Regional perspectives on climate change. MIT Press, Cambridge, p 171–223

Hassink J (1994) Effects of soil texture and grassland management on soil organic C and N and rates of C and N mineralization. Soil Biol Biochem 26:1221–1231

Hunt HW, Trlica MJ, Redente EF, Moore JC, Detling JK, Kittel TGF, Walter DE, Fowler MC, Klein DA, Elliott ET (1991) Simulation model for the effects of climate change on temperate grassland ecosystems. Ecol Model 53:205–246

Idso KE, Idso SB (1994) Plant responses to atmospheric CO_2 enrichment in the face of environmental constraints: a review of the past 10 years' research. Agric For Meteorol 69:153–203

IPCC (2000) Land use, land-use change, and forestry. A special report of the Intergovernmental Panel on Climate Change. Cambridge University Press, Cambridge

Melillo JM, McGuire AD, Kicklighter DW, Moore B III, Vorosmarty CJ, Schloss AL (1993) Global climate change and terrestrial net primary production. Nature 363:234–240

Nösberger J, Blum H, Fuhrer J (2000) Productive grasslands. In: Reddy KR, Hodges HF (eds) Global change and global crop productivity. CABI Publishing, CAB International, Wallingford, p 271–291

Ojima DS, Parton WJ, Schimel DS, Scurlock JMO, Kittel TGF (1993) Modeling the effects of climatic and CO_2 changes on grassland storage of soil C. Water Air Soil Pollut 70: 643–657

Pan Y, McGuire AD, Kicklighter DW, Melillo JM (1996) The importance of climate and soils for estimates of net primary production: a sensitivity analysis with the terrestrial ecosystem model. Global Change Biol 2:5–23

Parton WJ, Ojima DS, Schimel DS (1994) Environmental change in grasslands: assessment using models. Clim Change 28:111–141

Peterer R (1985) Ertragskundliche Untersuchungen von gedüngten Mähwiesen der subalpinen Stufe bei Davos. Veröffentlichungen des Geobotanischen Institutes der ETH, Heft 84, Stiftung Rübel, Zürich

Peyer K, Frei E (1992) Klassifikation der Böden der Schweiz: Profiluntersuchung, Klassifikationssystem, Definitionen der Begriffe, Anwendungsbeispiele. Eidgenössische Forschungsanstalt für landwirtschaftlichen Pflanzenbau, Zürich-Reckenholz

Prasuhn V, Braun M (1994) Abschätzung der Phosphor- und Stickstoffverluste aus diffusen Quellen in die Gewässer des Kantons Bern. Schriftenreihe der FAC 17. Swiss Federal Research Station for Agricultural Chemistry and Environmental Hygiene, Liebefeld-Bern

Rastetter EB, Agren GI, Shaver GR (1997) Responses of N-limited ecosystems to increased CO_2: a balanced-nutrition, coupled-element-cycle model. Ecol Appl 7: 444–460

Riedo M, Gyalistras D, Grub A, Rosset M, Fuhrer J (1997) Modelling grassland responses to climate change and elevated CO_2. Acta Oecol 18:305–311

Riedo M, Grub A, Rosset M, Fuhrer J (1998) A pasture simulation model for dry matter production, and fluxes of carbon, nitrogen, water and energy. Ecol Model 105:141–183

Riedo M, Gyalsitras D, Fuhrer J (1999) Using an ecosystem model linked to GCM-derived local weather scenarios to analyse effects of climate change and elevated CO_2 on dry matter production and partitioning, and water use in temperate managed grasslands. Global Change Biol 5: 213–223

Riedo M, Gyalistras D, Fuhrer J (2000) Net primary production and carbon stocks in differently managed grasslands: simulation of site-specific sensitivity to an increase in atmospheric CO_2 and to climate change. Ecol Model 134: 207–227

Rosset M, Riedo M, Grub A, Geissmann M, Fuhrer J (1997) Seasonal variation in radiation and energy balances of permanent pastures at different altitudes. Agric For Meteorol 86:245–258

Rounsvell MDA, Brignall AP, Siddoms PA (1996) Potential climate change effects on the distribution of agricultural grassland in England and Wales. Soil Use Manage 12: 44–51

Schönenberger W, Frei W (1988) Untersuchungen zur Ökologie und Technik der Hochlagenaufforstung — Forschungsergebnisse aus dem Lawinenanrissgebiet Stillberg. Schweiz Z Forstwirtsch 139:737–820

Statistical Sciences (1995) S-PLUS guide to statistical and mathematical analysis, Version 3.3. StatSci, MathSoft, Inc, Seattle, WA

Thornley JHM, Cannell MGR (1997) Temperate grassland responses to climate change: an analysis using the Hurley Pasture Model. Ann Bot 80:205–221

Tian H, Melillo JM, Kicklighter DW, McGuire AD, Helfrich J (1999) The sensitivity of terrestrial carbon storage to historical climate variability and atmospheric CO_2 in the United States. Tellus 51B:414–452

Von Wyl B (1987) Beitrag naturnaher Nutzungsformen zur Stabilisierung von Ökosystemen im Berggebiet, insbesondere zur Verhinderung von Bodenerosion. Schweiz Landwirtsch Forsch 26:405–464

Wildi O, Ewald K (eds) (1986) Der Naturraum und dessen Nutzung im alpinen Tourismusgebiet von Davos. Ergebnisse des MAB-Projektes Davos. Bericht 289, Eidg Anstalt für das forstliche Versuchwesen, Birmensdorf

Editorial responsibility: Hans von Storch, Geesthacht, Germany

Submitted: August 14, 2000; Accepted: March 9, 2001
Proofs received from author(s): June 29, 2001